# Periodic Load Estimation of a Wind Turbine Tower using a Model Demodulation Transformation

Pamososuryo, A.K.; Mulders, S.P.; Ferrari, Riccardo M.G.; van Wingerden, J.W.

**DOI**
10.23919/ACC53348.2022.9867768

**Publication date**
2022

**Document Version**
Final published version

**Published in**
Proceedings of the American Control Conference (ACC 2022)

2022 American Control Conference (ACC)
Atlanta, USA, June 8-10, 2022

# Periodic Load Estimation of a Wind Turbine Tower using a Model Demodulation Transformation

Atindriyo Kusumo Pamososuryo[1], Sebastiaan Paul Mulders[1], Riccardo Ferrari[1] and Jan-Willem van Wingerden[1]

***Abstract*— The ever-increasing power capacities of wind turbines promote the use of tall and slender turbine towers. This poses a challenge from a fatigue loading perspective by the relocation of the first and lightly-damped tower side-side natural frequency into the turbine operating regime, promoting its excitation during nominal operation. The excitation of this resonance can be aggravated by periodic loading in the presence of rotor mass and/or aerodynamic imbalance. Earlier work already presented a method to prevent the side-side excitation using a combination of model demodulation and quasi-linear parameter varying model predictive control techniques. However, the method does not incorporate features for active control for side-side load mitigations. Because the information of the beforementioned periodic side-side loading is unknown and unmeasurable in practical scenarios, this paper presents a Kalman filtering method for its estimation in a demodulated fashion. The Kalman filter employs an extended demodulated wind turbine model augmented with random walk models of the periodic load. The simulation result demonstrates the effectiveness of the proposed method in estimating the periodic load components along with unmeasurable tower states in their demodulated form. These estimates pose an opportunity for use in future advanced controller designs for active load reductions.**

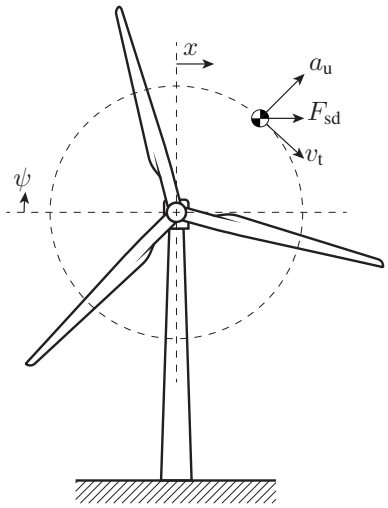


Fig. 1. A wind turbine excited at the side-side direction by a periodic load due to the rotor imbalance $F_{\mathrm{sd}}(t) = a_{\mathrm{u}} \cos(\psi(t))$ at the 1P frequency. The tangential speed of the periodic load is indicated by $v_{\mathrm{t}}$, and $x$ denotes tower top displacement in the horizontal direction.

## I. Introduction

A prevalent strategy to achieve cost-competitive wind energy generation systems is to upscale wind turbine sizes. Having taller tower and longer blade designs allow wind turbines to, respectively, access higher wind speeds and have a greater rotor swept area, such that more wind energy can be harnessed [1].

Taller turbines towers are typically more flexible due to decreased wall thickness, which could impose fatigue loading challenges [2]. Such towers can be excited more easily and severely as their first natural frequency may enter the rotor operating regime. The risk of resonance by the once-per-revolution (1P) frequency (i.e., the rotor rotational frequency) is thus becoming more prominent, particularly in the side-side direction as the aerodynamic damping is negligible [1]. Fig. 1 shows that a rotor mass and/or aerodynamic imbalance can form a persistent *periodic load/disturbance*, possibly exciting and exacerbating the side-side resonance [3].

To prevent prolonged operation at the tower resonant frequency, a possible solution is to implement the so-called *frequency skipping* logic in the controller design by manipulation of generator torque [3], [4]. However, implementing such rotational speed exclusion method has no convenient and inherent way of tuning and can therefore significantly affect power production. This problem advocates the use of an advanced control method which can cater for the power maximization and fatigue load minimization trade-off.

Recently, such an advanced and novel quasi-linear parameter varying (qLPV) control framework has been developed incorporating the aforementioned frequency skipping strategy with the capability to address the power-fatigue trade-off [5]. In this framework, a *model demodulation transformation*, brought from the field of precision mechatronics [6], is used to extract a slow-varying content of a signal from its higher-frequency *carrier*. In the previous work, the model demodulation method is applied to transform the wind turbine tower dynamics, so as to obtain an affine qLPV model scheduled on the rotor rotational frequency. The result enabled the use of a computationally attractive qLPV model predictive control (MPC) algorithm [7] by virtue of the obtained convex optimal control problem.

Frequency-skipping control prevents operation in a critical rotational speed range for extended periods of time. Still, load mitigation capabilities could be further enhanced by incorporating active damping features in the same qLPV-MPC

[1]Delft University of Technology, Delft Center for Systems and Control, Mekelweg 2, 2628 CD Delft, The Netherlands. {A.K.Pamososuryo, S.P.Mulders, R.Ferrari, J.W.vanWingerden}@tudelft.nl.

framework, thus rejecting the periodic load. The estimation of the periodic disturbance via demodulation would benefit the realization of such an active load control framework. The development of unknown input observer to estimate the demodulated load is the main contribution of this paper.

To aid the former mentioned estimation of demodulated disturbance, a demodulated system description of the tower side-side dynamics, extended from [5], is provided in this work. Specifically, the extended model description now includes (i) both the slowly-varying periodic excitation amplitude and phase offset; (ii) the effect of the generator torque to the tower motion; and (iii) the demodulated tower acceleration in the output equation. Based on this model, we propose a Kalman filter (KF) design, in which *random walk* models of the unknown periodic load components are augmented to the state equation. This allows their estimates to be obtained alongside the unmeasurable tower states, such as velocity and displacement, in a demodulated manner. Future control methods may benefit from the estimates by active load mitigations induced by the periodic disturbance, e.g., in the predictive framework of [5].

The remainder of this paper is structured as follows. Section II describes the nominal wind turbine dynamics, comprising that of the tower side-side motion and the drivetrain. Section III revisits the demodulated wind turbine model derivation along with its extension. The proposed KF design is elaborated upon in Section IV, the performance of which is examined in several case studies in Section V along with the validation of the extended model. Finally, in Section VI, conclusions are drawn and future prospects for active damping control purposes are given.

## II. Nominal Wind Turbine Model

The dynamics of a wind turbine tower are often described as a second-order mass-spring-damper system with a forcing term, and are given by the following state equation

$$\begin{bmatrix}\dot{x}_1(t)\\ \dot{x}_2(t)\end{bmatrix} = \begin{bmatrix}-d/m & -k/m\\ 1 & 0\end{bmatrix}\begin{bmatrix}x_1(t)\\ x_2(t)\end{bmatrix} + \begin{bmatrix}1/m\\ 0\end{bmatrix} F_{\mathrm{sd}}(t)\,, \quad (1)$$

where $m$, $d$, and $k$, are the (first) modal mass, damping, and stiffness of the tower in the side-side direction, respectively. The tower top velocity and displacement are respectively represented by $x_1$ and $x_2$. The symbol $t$ denotes the quantities of the fast-varying time scale as explained in the next section, and the $\dot{(\cdot)}$-notation indicates the first time-derivative of the specified signal.

The side-side force $F_{\mathrm{sd}}$ in (1) (and Fig. 1) is originally considered to be purely affected by a centrifugal force in the work of Mulders, et al. [5] and modeled as the following periodic signal

$$F_{\mathrm{sd}}(t) = a_{\mathrm{u}} \cos\left(\psi(t)\right), \quad (2)$$

with $a_u$ as the (constant) magnitude of the excitation. The rotor azimuth $\psi$ is defined as the angular travel of the first blade with respect to its vertically upward position. Note that the relation $\psi(t) = \int \omega_{\mathrm{r}}(t)\,\mathrm{d}t$ holds, with $\omega_{\mathrm{r}}$ as the angular velocity of the rotor, which determines the frequency of the periodic excitation.

**Remark 1.** *Although $F_{\mathrm{sd}}$ in (2) only contains a periodic load, this does not imply that other forcing effects, such as those static in nature, cannot be accounted for. That is, $F_{\mathrm{sd}}$ is considered as a generic force throughout this work.*

**Remark 2.** *The tower states $x_1$ and $x_2$, as well as their time derivatives, can be decomposed into their slow- and fast-varying components, as will be made clearer in the next section. The former exhibits quasi-steady state behavior, whereas this is not the case with the latter, especially if persistent periodic loading affects the system.*

The tower dynamics are augmented with the following simplified representation of the complete drivetrain dynamics

$$\dot{\omega}_{\mathrm{r}}(t) = \frac{T_{\mathrm{a}}(t) - GT_{\mathrm{g}}(t)}{J_{\mathrm{r}}}\,, \quad (3)$$

where $J_{\mathrm{r}}$, $G$, and $T_{\mathrm{g}}$ are the low-speed-shaft (LSS) equivalent inertia, gearbox ratio ($\geq 1$) and generator torque, respectively. The aerodynamic torque is defined as

$$T_{\mathrm{a}}(t) = \frac{1}{2}\rho_{\mathrm{a}}\pi R^3 C_{\mathrm{q}}(\omega_{\mathrm{r}}(t), v(t), \beta(t))v(t)^2\,,$$

with $\rho_{\mathrm{a}}$, $R$, $C_{\mathrm{q}}$, $v$, and $\beta$ as the air density, rotor radius, aerodynamic torque coefficient, wind speed, and pitch angle, respectively.

**Assumption 1.** *Throughout this study, the perfect knowledge of the aerodynamic torque $T_{\mathrm{a}}$ and wind speed $v$ is assumed since this paper focuses on estimating the unknown periodic disturbance; in realistic scenarios, these quantities can be estimated by an observer [8].*

## III. Extended Demodulated Model

The concept of model demodulation transformation was originally formulated to overcome the challenges surrounding the derivation of transient dynamic model of cantilevers in tapping mode atomic force microscopy (TM-AFM) [6]. The transformation is able to separate the slow- and fast-varying components of the states in a standard state-space form, thereby facilitating (model-based) controller design. The reader is referred to the work of Keyvani, et al. [6] for an extensive explanation and derivation of the model demodulation technique with an application to TM-AFM.

The technique was subsequently adopted by Mulders, et al. [5] to model the wind turbine tower dynamics in a demodulated fashion, enabling frequency skipping control capabilities in a predictive control framework. This section first revisits the model demodulation transformation, and secondly proposes extensions by the inclusion of generator torque signal affecting the tower side-side motion, and derives an output equation incorporating tower acceleration components and rotor speed.

The following key assumption underlies model demodulation [6].

**Assumption 2.** *The changes in the amplitude and phase of the system's response are much slower than a single oscillation cycle $T_\mathrm{r} \triangleq 2\pi/\omega_\mathrm{r}$. Accordingly, signals of slow time-varying time scale are indicated with the notation $\tau$, whereas its fast-varying counterpart with $t$.*

As per the above assumption, variables belonging to the slow time scale can be treated as constant over $T_\mathrm{r}$ such that

$$\int_0^{T_\mathrm{r}} f(\tau)g(t)\,\mathrm{d}t = f(\tau)\int_0^{T_\mathrm{r}} g(t)\,\mathrm{d}t\,,$$

$f$ and $g$ being generic variables at different time scales.

Using Euler's formula $e^{\mathrm{j}\sigma} = \cos(\sigma) + \mathrm{j}\sin(\sigma)$, the state variables of the wind turbine can be written as

$$\begin{aligned} x_i(t) &= a_i(\tau)\cos(\omega_\mathrm{r}(\tau)t + \phi_i(\tau))\,, \\ \Leftrightarrow x_i(t) &= \Re\{X_i(\tau)e^{\mathrm{j}\omega_\mathrm{r}(\tau)t}\}\,, \end{aligned} \tag{4}$$

with $X_i(\tau) = a_i(\tau)e^{\mathrm{j}\phi_i(\tau)} \in \mathbb{C}$, where the subscript $i$ is an index. The $\Re\{\cdot\}$-notation corresponds to the real component of the considered variable, while the $\Im\{\cdot\}$-notation refers to that of the imaginary part, as used later on in the derivation. Note that to reconstruct the signal's amplitude and phase offset, the following relations are used respectively

$$a_i(\tau) = \sqrt{\Re\{X_i(\tau)\}^2 + \Im\{X_i(\tau)\}^2}\,, \tag{5}$$

$$\phi_i(\tau) = \arctan\left(\Im\{X_i(\tau)\}/\Re\{X_i(\tau)\}\right). \tag{6}$$

The first time-derivative of (4) is given by

$$\dot{x}_i(t) = \Re\left\{\left(\dot{X}_i(\tau) + \mathrm{j}\omega_\mathrm{r}(\tau)X_i(\tau)\right)e^{\mathrm{j}\omega_\mathrm{r}(\tau)t}\right\}. \tag{7}$$

The side-side force in (2) is extended to include an unknown slow time-varying phase offset of the periodic load $\phi_\mathrm{u}$ since, in reality, the load might not be in-phase with the rotor azimuth. Moreover, $a_\mathrm{u}$ is now considered to be slowly-varying rather than a constant; further generalizing the periodic load characteristic. By adding the contribution of $T_\mathrm{g}$ in the form of a static contribution to the tower dynamics, the side-side force becomes

$$F_{\mathrm{sd,ext}}(t) = a_\mathrm{u}(\tau)\cos\left(\omega_\mathrm{r}(\tau)\,t + \phi_\mathrm{u}(\tau)\right) + c\,T_\mathrm{g}(t)\,, \tag{8}$$

thereby extending the side-side force as formulated in [5]. The scaling factor $c = 3/2H$ represents the ratio between angular and translational displacement of the tower motion, here assumed as a prismatic beam [9], with $H$ being the tower height.

The demodulation of the side-side force is performed by considering it as a *semi-periodic signal*, i.e., a harmonic signal with slowly varying amplitude and phase. Broken down into its *semi-harmonic components* in a similar fashion as (4), (8) can be rewritten as follows

$$F_{\mathrm{sd,ext}}(t) = \Re\left\{A_\mathrm{u}(\tau)e^{\mathrm{j}\omega_\mathrm{r}(\tau)t} + c\sum_{n=0}^{\infty}\mathrm{T}_\mathrm{g}^{(n)}(\tau)e^{\mathrm{j}n\omega_\mathrm{r}(\tau)t}\right\}, \tag{9}$$

with $A_\mathrm{u}(\tau) = a_\mathrm{u}(\tau)e^{\mathrm{j}\phi_\mathrm{u}(\tau)} \in \mathbb{C}$ representing the slow-varying component of the periodic load signal. The amplitude and phase of the $n$-th harmonic component of the generator torque signal is denoted by $\mathrm{T}_\mathrm{g}^{(n)}(\tau) \in \mathbb{C}$.

Substituting (4), (7), and (9) into (1) yields the relations

$$\begin{aligned} \Re\Bigg\{\Bigg(&\dot{X}_1(\tau) + \mathrm{j}\omega_\mathrm{r}(\tau)X_1(\tau) + \frac{d}{m}X_1(\tau) + \frac{k}{m}X_2(\tau) \\ &-\frac{1}{m}A_\mathrm{u}(\tau)\Bigg)e^{\mathrm{j}\omega_\mathrm{r}(\tau)t} - \frac{c}{m}\sum_{n=0}^{\infty}\mathrm{T}_\mathrm{g}^{(n)}(\tau)e^{\mathrm{j}n\omega_\mathrm{r}(\tau)t}\Bigg\} = 0\,, \end{aligned} \tag{10}$$

and

$$\Re\left\{\left(\dot{X}_2(\tau) + \mathrm{j}\omega_\mathrm{r}(\tau)X_2(\tau) - X_1(\tau)\right)\mathrm{e}^{\mathrm{j}\omega_\mathrm{r}(\tau)t}\right\} = 0\,. \tag{11}$$

Multiplying both sides of (10) and (11) with $e^{\mathrm{j}\omega_\mathrm{r}(\tau)t}$ and integrating over an oscillation period $\int_0^{T_\mathrm{r}}(\cdot)\mathrm{e}^{\mathrm{j}\omega_\mathrm{r}(\tau)t}\,\mathrm{d}t$ results in the following projections into the space of the first harmonic component

$$\begin{aligned} \int_0^{T_\mathrm{r}}\Re\Bigg\{\Bigg(&\dot{X}_1(\tau) + \mathrm{j}\omega_\mathrm{r}(\tau)X_1(\tau) + \frac{d}{m}X_1(\tau) + \frac{k}{m}X_2(\tau) \\ &-\frac{1}{m}A_\mathrm{u}(\tau) - \frac{c}{m}\mathrm{T}_\mathrm{g}^{(1)}(\tau)\Bigg)e^{\mathrm{j}\omega_\mathrm{r}(\tau)t}\Bigg\}\mathrm{e}^{\mathrm{j}\omega_\mathrm{r}(\tau)t}\,\mathrm{d}t = 0\,, \end{aligned} \tag{12}$$

and

$$\begin{aligned} \int_0^{T_\mathrm{r}}\Re\Big\{\Big(&\dot{X}_2(\tau) + \mathrm{j}\omega_\mathrm{r}X_2(\tau) \\ &-\ X_1(\tau)\Big)\mathrm{e}^{\mathrm{j}\omega_\mathrm{r}(\tau)t}\Big\}\mathrm{e}^{\mathrm{j}\omega_\mathrm{r}(\tau)t}\,\mathrm{d}t = 0\,. \end{aligned} \tag{13}$$

It is important to note that in (12), due to the following orthogonality property of harmonic functions

$$\int_0^{2\pi}\Re\{\gamma e^{\mathrm{j}n\theta}\}e^{\mathrm{j}\theta}\mathrm{d}\theta = 0,\ \forall\ n \neq 1\,, \tag{14}$$

only the first harmonic of $\mathrm{T}_g^{(n)}$, that is $\mathrm{T}_g^{(1)}$, is left in the equation while those corresponding to zeroth and higher harmonics are cancelled.

Another orthogonality property of harmonic functions which can be exploited is

$$\int_0^{2\pi}\Re\{\gamma e^{\mathrm{j}\theta}\}e^{\mathrm{j}\theta}\mathrm{d}\theta = 0,\ \text{iff}\,\gamma \in \mathbb{C} = 0\,, \tag{15}$$

by which the following state equation is obtained

$$\begin{bmatrix}\dot{X}_1\\ \dot{X}_2\end{bmatrix} = \begin{bmatrix}-\mathrm{j}\omega_\mathrm{r} - \frac{d}{m} & -\frac{k}{m}\\ 1 & -\mathrm{j}\omega_\mathrm{r}\end{bmatrix}\begin{bmatrix}X_1\\ X_2\end{bmatrix} + \begin{bmatrix}\frac{1}{m} & \frac{c}{m}\\ 0 & 0\end{bmatrix}\begin{bmatrix}A_\mathrm{u}\\ \mathrm{T}_\mathrm{g}^{(1)}\end{bmatrix}, \tag{16}$$

with $\omega_\mathrm{r}$ as the scheduling variable. For the sake of simplicity, the notation $\tau$ is dropped in the above equation and for the remainder of this paper.

### A. Extended Demodulated State Equation

As a step toward obtaining a qLPV representation of the combined drivetrain and demodulated tower dynamics, (16) is augmented with (3). However, it is important to realize that this equation contains several complex terms, hindering it from being directly usable for control system designs. Therefore, the equation is rewritten by separating the real or imaginary parts by defining the new states $q_1 = \Re\{X_1\} \in \mathbb{R}$, $q_2 = \Im\{X_1\} \in \mathbb{R}$, $q_3 = \Re\{X_2\} \in \mathbb{R}$, and $q_4 = \Im\{X_2\} \in \mathbb{R}$,

forming the following extension of the demodulated state equation with respect to that of Mulders, et al. [5]

$$\underbrace{\begin{bmatrix}\dot{q}_1\\ \dot{q}_2\\ \dot{q}_3\\ \dot{q}_4\\ \dot{\omega}_\mathrm{r}\end{bmatrix}}_{\dot{\mathbf{x}}} = \underbrace{\begin{bmatrix}-\frac{d}{m} & \omega_\mathrm{r} & -\frac{k}{m} & 0 & 0\\ -\omega_\mathrm{r} & -\frac{d}{m} & 0 & -\frac{k}{m} & 0\\ 1 & 0 & 0 & \omega_\mathrm{r} & 0\\ 0 & 1 & -\omega_\mathrm{r} & 0 & 0\\ 0 & 0 & 0 & 0 & 0\end{bmatrix}}_{\mathbf{A}(\rho)} \underbrace{\begin{bmatrix}q_1\\ q_2\\ q_3\\ q_4\\ \omega_\mathrm{r}\end{bmatrix}}_{\mathbf{x}} + \underbrace{\begin{bmatrix}\frac{c}{m} & 0 & 0\\ 0 & \frac{c}{m} & 0\\ 0 & 0 & 0\\ 0 & 0 & 0\\ 0 & 0 & \frac{1}{J_\mathrm{r}}\end{bmatrix}}_{\mathbf{B}_\mathrm{u}} \underbrace{\begin{bmatrix}\Re\{\mathrm{T}_\mathrm{g}^{(1)}\}\\ \Im\{\mathrm{T}_\mathrm{g}^{(1)}\}\\ T_\mathrm{a}-GT_\mathrm{g}\end{bmatrix}}_{\mathbf{u}} + \underbrace{\begin{bmatrix}\frac{1}{m} & 0\\ 0 & \frac{1}{m}\\ 0 & 0\\ 0 & 0\end{bmatrix}}_{\mathbf{B}_\mathrm{d}} \underbrace{\begin{bmatrix}\Re\{A_\mathrm{u}\}\\ \Im\{A_\mathrm{u}\}\end{bmatrix}}_{\mathbf{d}}, \tag{17}$$

with the symbols $\mathbf{x}$, $\mathbf{u}$, and $\mathbf{d}$ referring to the state, input, and disturbance vectors. $\mathbf{A}(\rho)$, $\mathbf{B_u}$, and $\mathbf{B_d}$ are the (parameter-dependent) state, input, and disturbance matrices, respectively, with the scheduling variable $\rho = \omega_\mathrm{r}$.

### B. Output Equation Derivation

Following the derivation of the new state equation, the output of the demodulated wind turbine model may now be defined. In [5], the output was chosen as the displacement signal, following [6]. However, in reality, this signal is unavailable from the wind turbine measurements. In this work, a step toward obtaining a more realistic model is taken by defining the demodulated acceleration signal, which was not discussed in [5], [6], as the new output.

The acceleration signal in the demodulated fashion is calculated according to (7) for $i = 1$ as follows

$$q_a + \mathrm{j}q_b = \dot{X}_1 + \mathrm{j}\omega_\mathrm{r}X_1\,, \tag{18}$$

with $q_a = \Re\{\dot{X}_1 + \mathrm{j}\omega_\mathrm{r}X_1\} \in \mathbb{R}$ and $q_b = \Im\{\dot{X}_1 + \mathrm{j}\omega_\mathrm{r}X_1\} \in \mathbb{R}$. By substitution of $\dot{X}_1$ from the state equation (16) into (18), the demodulated acceleration is obtained. Appending $\omega_\mathrm{r}$ as another output, the final output equation is thus

$$\underbrace{\begin{bmatrix}q_a\\ q_b\\ \omega_\mathrm{r}\end{bmatrix}}_{\mathbf{y}} = \underbrace{\begin{bmatrix}-\frac{d}{m} & 0 & -\frac{k}{m} & 0 & 0\\ 0 & -\frac{d}{m} & 0 & -\frac{k}{m} & 0\\ 0 & 0 & 0 & 0 & 1\end{bmatrix}}_{\mathbf{C}} \underbrace{\begin{bmatrix}q_1\\ q_2\\ q_3\\ q_4\\ \omega_\mathrm{r}\end{bmatrix}}_{\mathbf{x}} + \underbrace{\begin{bmatrix}\frac{c}{m} & 0 & 0\\ 0 & \frac{c}{m} & 0\\ 0 & 0 & 0\end{bmatrix}}_{\mathbf{D}_\mathrm{u}} \underbrace{\begin{bmatrix}\Re\{\mathrm{T}_\mathrm{g}^{(1)}\}\\ \Im\{\mathrm{T}_\mathrm{g}^{(1)}\}\\ T_\mathrm{a}-GT_\mathrm{g}\end{bmatrix}}_{\mathbf{u}} + \underbrace{\begin{bmatrix}\frac{1}{m} & 0\\ 0 & \frac{1}{m}\\ 0 & 0\end{bmatrix}}_{\mathbf{D}_\mathrm{d}} \underbrace{\begin{bmatrix}\Re\{A_\mathrm{u}\}\\ \Im\{A_\mathrm{u}\}\end{bmatrix}}_{\mathbf{d}}. \tag{19}$$

The output vector and matrix are denoted by $\mathbf{y}$ and $\mathbf{C}$ and the feedthrough matrices $\mathbf{D}_\mathrm{u}$ and $\mathbf{D}_\mathrm{d}$ correspond to that of the system's inputs and disturbances, respectively.

### C. Measurement Signal Demodulation

In the real wind turbine system, measurement signals (e.g., tower acceleration), as well as control inputs, (e.g., generator torque), are not presented in their demodulated form. Hence, these signals need to be processed by a *measurement signal demodulation* (MSD) such that their 1P component can be obtained and used with the extended demodulated model derived in the preceding sections. Here, the method for demodulating measurement signal as presented by Bottasso, et al. [10] is employed and briefly summarized in the following. For further details, please consult [10].

The demodulation of a discrete signal $\hat{z}(t_k)$ with $t_k = k\Delta t$ over $N_\mathrm{R}$ revolutions is expressed as

$$\hat{z}(t_k) = \hat{z}(\psi(t_k)) \approx z_K^0 + \sum_{n=1}^{N_\mathrm{B}} \Big( z_{c,K}^{(n)} \cos\left(n\psi(t_k)\right) + z_{s,K}^{(n)} \sin\left(n\psi(t_k)\right) \Big)\,,$$

with $N_\mathrm{B}$ as harmonic bases, angular position $\psi(t_k) \in [\psi_K - 2\pi N_\mathrm{R}, \psi_K]$, where $\psi_K = K\Delta\psi$ and the coefficients are calculated by the following integral operations

$$\begin{aligned} z_{c,K}^{(n)} &= \frac{1}{\pi N_\mathrm{R}} \int_{\psi_K - 2\pi N_\mathrm{R}}^{\psi_K} \hat{z}(\psi)\cos\left(n\psi\right)\mathrm{d}\psi\,,\\ z_{s,K}^{(n)} &= \frac{1}{\pi N_\mathrm{R}} \int_{\psi_K - 2\pi N_\mathrm{R}}^{\psi_K} \hat{z}(\psi)\sin\left(n\psi\right)\mathrm{d}\psi\,. \end{aligned} \tag{20}$$

which can be approximated, e.g., by using trapezoidal numerical integration. The $\hat{(\cdot)}$-notation is used to represent the estimate of the specified signal. The azimuthal sampling (i.e., sampling at different azimuth positions) is represented by $\Delta\psi$, whose steps are indicated by $K$ *spatial* steps. Meanwhile, $\Delta t$ denotes sampling time whose *temporal* steps are indicated by $k$. In this paper, note that only the first harmonic components of (20), referring to the 1P frequency, are used.

## IV. Kalman Filter Design

Kalman filtering is employed to retrieve information about the unknown periodic load, as well as the wind turbine states unavailable from the measurements. The KF is defined by the following discretized state-space equation—augmented with the random walk models of the disturbance [11]

$$\begin{aligned} \underbrace{\left[\begin{array}{c}\mathbf{x}_{k+1}\\ \hline \mathbf{d}_{k+1}\end{array}\right]}_{\mathbf{x}_{\mathrm{aug},k+1}} &= \underbrace{\left[\begin{array}{c|c}\mathcal{A}(\rho_k) & \mathcal{B}_\mathrm{d}\\ \hline \mathbf{0} & \mathbf{I}\end{array}\right]}_{\mathcal{A}_\mathrm{aug}(\rho_k)} \underbrace{\left[\begin{array}{c}\mathbf{x}_k\\ \hline \mathbf{d}_k\end{array}\right]}_{\mathbf{x}_{\mathrm{aug},k}}\\ &\quad + \underbrace{\left[\begin{array}{c}\mathcal{B}_\mathrm{u}\\ \hline \mathbf{0}\end{array}\right]}_{\mathcal{B}_\mathrm{aug}} \mathbf{u}_k + \underbrace{\left[\begin{array}{c}\mathbf{w}_k\\ \hline \mathbf{w}_{\mathrm{d},k}\end{array}\right]}_{\mathbf{w}_{\mathrm{aug},k}}, \end{aligned} \tag{21}$$

$$\mathbf{y}_k = \underbrace{\left[\begin{array}{c|c}\mathbf{C} & \mathbf{D}_\mathrm{d}\end{array}\right]}_{\mathbf{C}_\mathrm{aug}} \mathbf{x}_{\mathrm{aug},k} + \mathbf{D}_\mathrm{u}\mathbf{u}_k + \mathbf{v}_k\,, \tag{22}$$

with $\mathcal{A}(\rho_k)$, $\mathcal{B}_\mathrm{u}$, and $\mathcal{B}_\mathrm{d}$ as the discretized state, input, and disturbance matrices, respectively. The quantities $\mathbf{w}$, $\mathbf{w}_d$, and $\mathbf{v}$ are the uncorrelated process, random walk, and measurement white noise sequence, the covariance matrix of which is defined as

$$E\begin{bmatrix}\mathbf{w}_{\mathrm{aug},k}\\ \mathbf{v}_k\end{bmatrix}\begin{bmatrix}\mathbf{w}_{\mathrm{aug},k}^T & \mathbf{v}_k^T\end{bmatrix} = \mathrm{diag}(\mathbf{Q}_\mathrm{aug}, \mathbf{R})\,, \tag{23}$$

TABLE I

PARAMETERS OF THE (MODIFIED) NREL-5MW REFERENCE WIND TURBINE.

| Description | Symbol | Value | Unit |
|---|---|---|---|
| Gearbox ratio | $G$ | 97 | - |
| LSS equivalent inertia | $J_{\mathrm{r}}$ | $4.0802\times10^{7}$ | kg m$^2$ |
| Rotor radius | $R$ | 63 | m |
| Tower height | $H$ | 90 | m |
| Tower modal mass | $m$ | 1000 | kg |
| Tower modal damping | $d$ | 100 | kg s$^{-1}$ |
| Tower modal stiffness | $k$ | 500 | kg s$^{-2}$ |
| Tower natural frequency | $\omega_{\mathrm{n}}$ | 0.7071 | rad s$^{-1}$ |

where the state covariance matrix $\mathbf{Q}_{\text{aug}}$ and the measurement covariance matrix $\mathbf{R}$ act as tuning variables for the KF. The operator $E$ represents the expected value. The KF algorithm includes two steps: *a priori* state and error covariance matrix estimation, followed by *a posteriori* state and error covariance matrix correction. For the detailed recursive algorithm, the interested reader is referred to [11].

## V. CASE STUDY

Prior to assessing the performance of the designed KF, it is compelling to validate the derived extended demodulated wind turbine model, as represented by the state equation (17) and output equation (19). After that, the ability of the KF in estimating the unknown periodic load components, as well as the tower velocity and displacement, is illustrated.

As a demonstration, the reference NREL 5MW wind turbine model [12] is considered. Its first tower modal properties, specified in Table I, are tuned such that its natural frequency $\omega_{\mathrm{n}} = \sqrt{k/m}$ lies in the below-rated operating region; resembling slender, *soft-soft* towers [2]. In this case, a conventional $K - \omega^2$ generator torque control law [1] is employed. Since above-rated turbine operation is of no interest in this study, a staircase uniform wind profile in the $v = 4 - 10$ m/s range is considered with 1.5 m/s step increases every 100 s, for 500 s of total simulation time.

### A. Model Validation

In this section, the response of the demodulated acceleration signal pair $\{q_a, q_b\}$ is demonstrated. In addition, the nominal model's measurement is demodulated using MSD, which yields the $\{q_c^{(1)}, q_s^{(1)}\}$ signals, i.e. the cosine and sine components of the first harmonic of the nominal tower acceleration signal. As depicted in Fig. 2, the amplitude of these signal pairs are calculated by taking their two-norms to show whether they follow the nominal model's amplitude. This is shown to be the case for both $\{q_a, q_b\}$ and $\{q_c^{(1)}, q_s^{(1)}\}$, although the latter shows a delayed response due to the integration in (20). Even though the phase information calculated from these pairs are not included in the figure, similar behavior is observed.

Hence, this result implies that the proposed extended demodulated model can be used in a more realistic situation as opposed to [5], where a demodulated second-order model is excited to provide tower displacement amplitude information. Moreover, the MSD method enables measurements to be

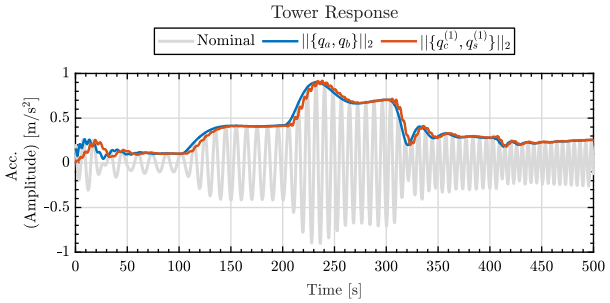


Fig. 2. Comparison between the measured nominal wind turbine tower acceleration and the amplitude of both the extended demodulated model and MSD-demodulated signals, $\{q_a, q_b\}$ and $\{q_c^{(1)}, q_s^{(1)}\}$, respectively. The demodulated responses show accurate tracking of the periodic amplitude, whereas those of the MSD-method exhibit a slight delay as a result of integral operations of the measurements demodulation.

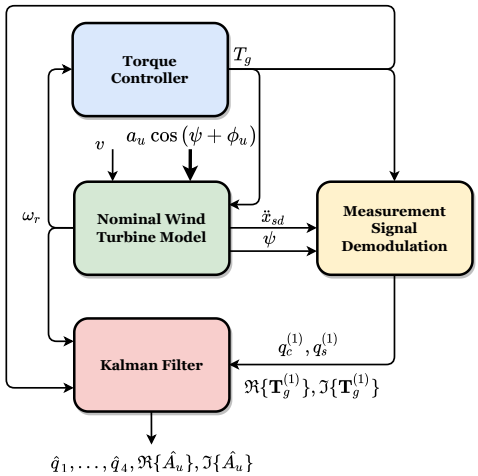


Fig. 3. Implementation the proposed KF based on the demodulated wind turbine and tower model. The KF estimates the demodulated periodic load components, as well as the unmeasurable tower states, and takes inputs from the torque controller and the (MSD-demodulated) nominal wind turbine model measurements.

demodulated and used together with the proposed model, such as for Kalman filtering in the following section.

### B. Kalman Filter Performance Assessment

In the performance assessment of the proposed periodic load estimation method, the extended demodulated model is employed as the internal model of the KF after discretized with fourth-order Runge-Kutta method at 0.01 s of sampling time. The observer takes the tower acceleration and the generator torque input in their MSD-demodulated forms, whereas the rotor measurement is fed directly from the turbine, as illustrated in Fig. 3.

The periodic load $a_{\mathrm{u}} \cos(\omega_{\mathrm{r}} t + \phi_{\mathrm{u}})$ with slowly-varying $a_{\mathrm{u}}$ and $\phi_{\mathrm{u}}$ is simulated by generating sinusoidal $\Re\{A_{\mathrm{u}}\}$ and $\Im\{A_{\mathrm{u}}\}$, with an amplitude of $75\sqrt{2} \pm 15$ N and a frequency of 0.025 rad/s. Imposing a phase offset of $\pi/2$ rad for $\Im\{A_{\mathrm{u}}\}$ generates a varying $\phi_{\mathrm{u}}$. The parameters of the resulting periodic signal can thus be characterized as $a_{\mathrm{u}} \in [135, 165]$ N and $\phi_{\mathrm{u}} \in [39.25, 50.75]$ deg. For the specified simulation settings, the covariance matrices are selected to be $\mathbf{Q}_{\text{aug}} = \mathrm{diag}(10^{-6}, \ldots, 10^{-6}, 5 \cdot 10^{-2}, 5 \cdot 10^{-2})$ and $\mathbf{R} = \mathrm{diag}(10^{-5}, 10^{-5}, 10^{-5})$.

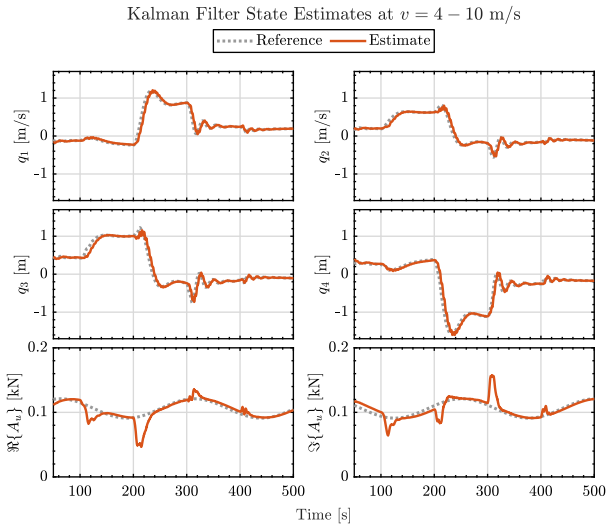


Fig. 4. Kalman filtering result. Good tracking of the estimates with respect to the reference periodic load components and tower states is observed despite slightly delayed response, bias, and transient discrepancies after each wind step.

The simulation results are shown in Fig. 4, demonstrating that the unknown wind turbine tower states $\hat{q}_1, \ldots, \hat{q}_4$ are reconstructed with minimal discrepancies from the reference. Moreover, the periodic disturbance elements $\Re\{A_\mathrm{u}\}$ and $\Im\{A_\mathrm{u}\}$ are estimated, from which the slowly-varied amplitude and phase offset can be calculated. They show good tracking behavior with respect to the original signal. In Fig. 5, the capability of the load amplitude estimate is compared with the original signal; demonstrating that the former is able to closely follow the latter's amplitude.

Discrepancies are seen after every step in wind speed before the estimates converge back to the actual signal. The MSD-demodulated signals experience some delay due to the integral operations in (20), which are shown to be more sensitive toward large, abrupt changes in the tower acceleration. This appeared to be the case particularly during the transients near the critical tower excitation at $t = 200$ s and $t = 300$ s (see Fig. 2). It is also observed that the steady state estimation error of $\Re\{A_\mathrm{u}\}$ varies for different wind speeds within $[0.5, 4.5]\%$ range whereas for $\Im\{A_\mathrm{u}\}$ this value ranges between $[0.3, 5]\%$. Such performance limitations might suggest that a delay-proof mechanism needs to be incorporated for future KF design. Regardless, it has been shown that using the MSD-demodulated acceleration signals as the KF inputs, the unknown periodic disturbance and the remaining demodulated tower states could be reconstructed to a large extent. This allows strategies, such as feedforward control [9], to be employed together with the state-of-the-art qLPV-MPC algorithm [5] in future work for further load reductions.

## VI. Conclusions

In this work, the extended demodulated wind turbine model has been derived, which incorporates slowly-varying periodic excitation's amplitude and phase offset, generator torque contribution to the tower motion, and a new output equation containing demodulated acceleration signal. The extended

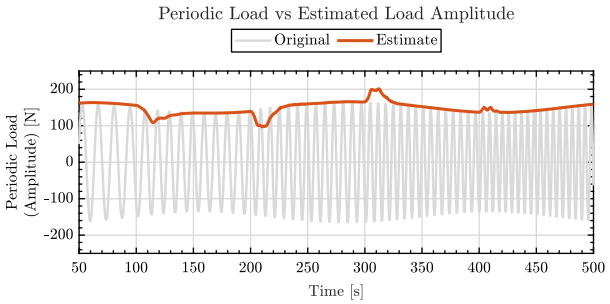


Fig. 5. Reconstruction of the periodic load amplitude from the KF estimation compared with the original signal.

model's output has been evaluated against that of the nominal signal, in which the former has been shown to closely track the amplitude of the latter. Furthermore, a Kalman filter augmented with random walk models has been designed using the new model and assessed at the below-rated regime. It proved capable of estimating the periodic disturbance components and the unknown tower states, in good agreement with the respective disturbance and tower states references. Future work will comprise improvements on the delay tolerance aspect of the unknown input observer, as well as active tower damping control by qLPV-MPC, by means of the extended model.

## References


[1] T. Burton, N. Jenkins, D. Sharpe, and E. Bossanyi, *Wind Energy Handbook*. Chichester, UK: John Wiley & Sons, Ltd, may 2011.

[2] K. Dykes, R. Damiani, O. Roberts, and E. Lantz, "Analysis of ideal towers for tall wind applications," National Renewable Energy Laboratory (NREL), Golden, Colorado, techreport NREL/CP-5000-70642, Jan. 2018.

[3] J. Licari, J. B. Ekanayake, and N. Jenkins, "Investigation of a speed exclusion zone to prevent tower resonance in variable-speed wind turbines," *IEEE Transactions on Sustainable Energy*, vol. 4, no. 4, pp. 977–984, 2013.

[4] E. A. Bossanyi, "Wind Turbine Control for Load Reduction," *Wind Energy*, vol. 6, no. 3, pp. 229–244, jul 2003.

[5] S. P. Mulders, T. G. Hovgaard, J. D. Grunnet, and J. W. van Wingerden, "Preventing wind turbine tower natural frequency excitation with a quasi-LPV model predictive control scheme," *Wind Energy*, vol. 23, no. 3, pp. 627–644, mar 2020.

[6] A. Keyvani, M. S. Tamer, J. W. van Wingerden, J. F. Goosen, and F. van Keulen, "A comprehensive model for transient behavior of tapping mode atomic force microscope," *Nonlinear Dynamics*, vol. 97, no. 2, pp. 1601–1617, 2019.

[7] P. S. G. Cisneros, S. Voss, and H. Werner, "Efficient Nonlinear Model Predictive Control via quasi-LPV representation," in *2016 IEEE 55th Conference on Decision and Control (CDC)*, no. Cdc. IEEE, dec 2016, pp. 3216–3221.

[8] Y. Liu, A. K. Pamososuryo, R. M. G. Ferrari, and J. W. van Wingerden, "The immersion and invariance wind speed estimator revisited and new results," *IEEE Control Systems Letters*, vol. 6, pp. 361–366, 2022.

[9] K. Selvam, S. Kanev, J. W. van Wingerden, T. van Engelen, and M. Verhaegen, "Feedback-feedforward individual pitch control for wind turbine load reduction," *International Journal of Robust and Nonlinear Control*, vol. 19, no. 1, pp. 72–91, jan 2009.

[10] C. Bottasso, A. Croce, C. Riboldi, and Y. Nam, "Multi-layer control architecture for the reduction of deterministic and non-deterministic loads on wind turbines," *Renewable Energy*, vol. 51, pp. 159–169, mar 2013.

[11] M. Verhaegen and V. Verdult, *Filtering and system identification: a least squares approach*. Cambridge university press, 2007.

[12] J. Jonkman, S. Butterfield, W. Musial, and G. Scott, "Definition of a 5-MW Reference Wind Turbine for Offshore System Development," National Renewable Energy Laboratory (NREL), Golden, CO, Tech. Rep., feb 2009.